Supporting information

Ionic liquid gated carbon nanotube saturable absorber for switchable pulse generation

Yuriy Gladush,[1] Aram A. Mkrtchyan,[1,2] Daria S. Kopylova,[1] Aleksey Ivanenko,[3] Boris Nyushkov,[3,4] Sergey Kobtsev,[3] Alexey Kokhanovskiy, [3] Alexander Khegai,[5] Mikhail Melkumov,[5] Maria Burdanova,[6] Michael Staniforth,[6] James Lloyd-Hughes,[6] Albert G. Nasibulin*[1,7]*

[1]Skolkovo Institute of Science and Technology, Moscow 121205, Russia

[2]Moscow Institute of Physics and Technology, Moscow region, Dolgoprudny 141700, Russia

[3]Novosibirsk State University, Novosibirsk 630090, Russia

[4]Novosibirsk State Technical University, Novosibirsk 630073, Russia

[5]Fiber Optic Research Center, Moscow 119333, Russia

[6]Department of Physics, University of Warwick, Coventry CV4 7AL, UK

[7]Aalto University, FI-00076 Aalto, Espoo, Finland

* y.gladush@skoltech.ru; a.nasibulin@skoltech.ru

S.1 Video

We provide an animation file that illustrates sample fabrication with three steps (see Figure 1 in the main text): 1) SWCNT deposition with dry transfer technique; 2) ionic liquid dripping; 3) sample encapsulation:

Sample fabrication.avi

S.2 Cyclic voltammetry

To examine the electric double layer formation on the SWCNT electrodes and its stability window we performed cyclic voltammetry measurements of the samples (Figure S1). For the scanning range ±2 V curves of several sweeps lie down on each other with a good precision in correspondence with double-layer capacitor behavior. For the encapsulated sample the shape of the curves changed only slightly after two months of heavy usage. Exceeding of the voltage stability window leads to nonreproducible behavior and degradation of the sample with reduction of voltage response.

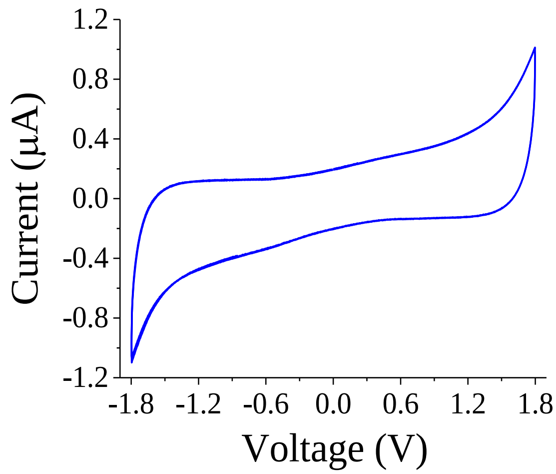

Figure S1. Current as a function of voltage in the cycling voltammetry experiment (100 mV/s sweep rate).

S.3 Transmittance spectra in vis-NIR range

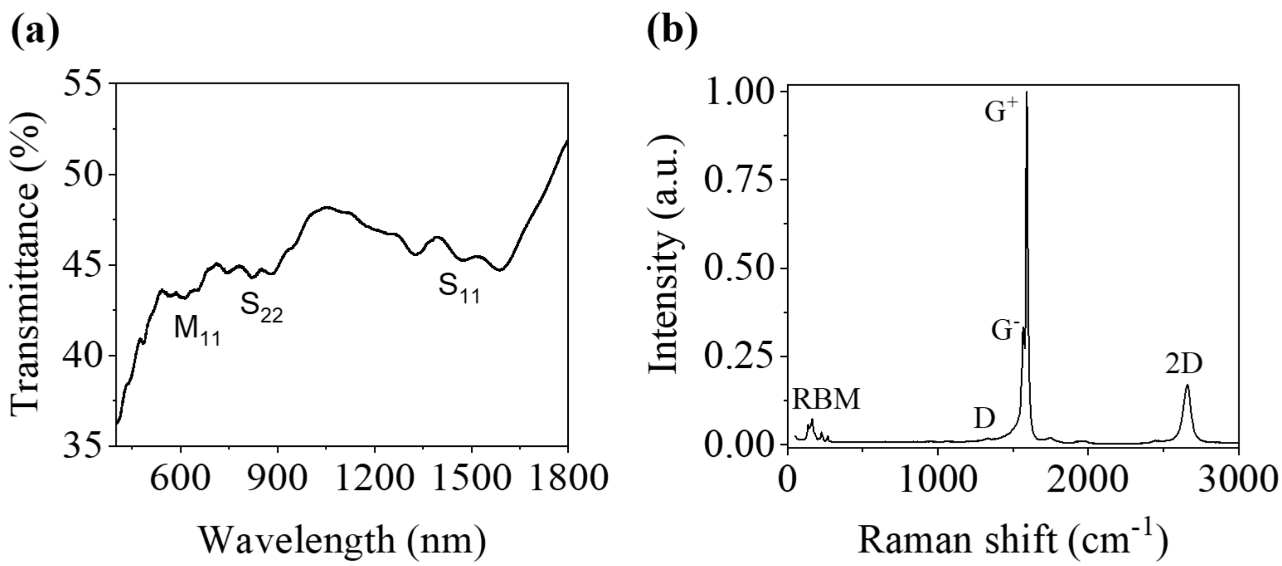

Figure S2. (a) Transmittance and (b) Raman spectra of a SWCNT film on a glass substrate.

In Figure S2 (a) the transmittance spectrum reveals a broad S_{11} transition in the spectral range of 1200 – 1700 nm. The smaller features on the broad transition line corresponds to the nonuniform chirality distribution of the as synthesized SWCNTs. Figure S2 (b) demonstrates Raman spectrum of the SWCNT film. G/D ratio exceeding one hundred evidence for a high quality of as synthesized SWCNTs.

S.4 Radiofrequency Spectra

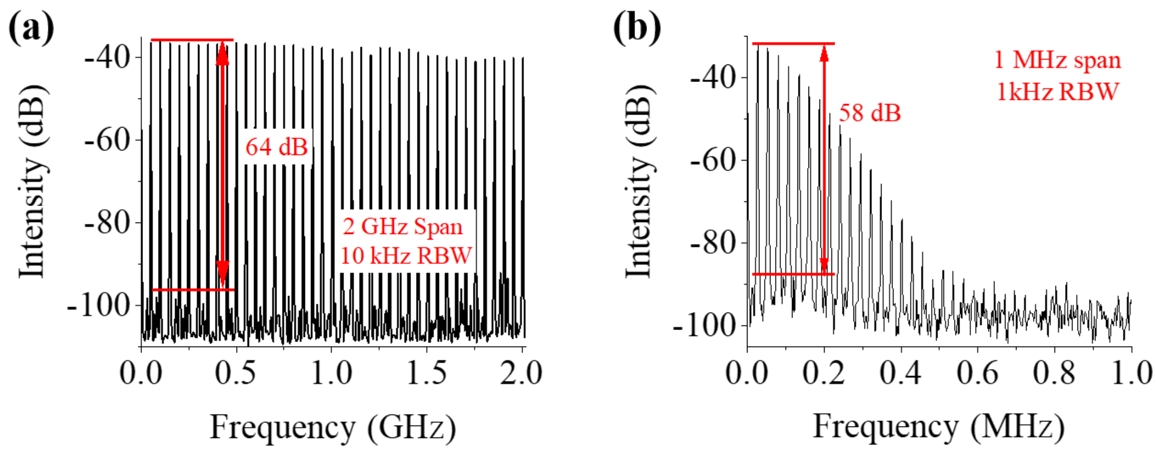

Figure S3. RF spectra of pulsed laser radiation obtained in (a) mode-locked regime and (b) Q-switched regime.

RF spectrum of the regular pulse train obtained in the mode-locked regime is shown in Figure S3 (a). Signal-to-noise ratio for the first harmonic reaches 64 dB. For the 40th harmonic of mode-locked pulses amplitude decreases only by 4 dB that proves the high quality of mode-locked regime. Figure S3 (b) demonstrates RF spectrum of pulse radiation obtained in the Q-switched regime.

S.5 Switching of the pulse regimes in Er-fibre laser based on non-PM single-mode fibers

In the following section we described the experiments on the pulse switching with the fiber laser without polarization maintaining. For this laser we prepared a SWCNT-SA sample based on the side-polished single-mode fiber (SMF). The sample was prepared the same way described in the main text of the paper. The transmittance for the in-plane and out-of-plane polarization under varied voltage is shown in Figure S4a. This sample showed a transmittance minimum shift to the positive voltage, so it was easier to apply negative voltages for an effective Fermi level manipulation.

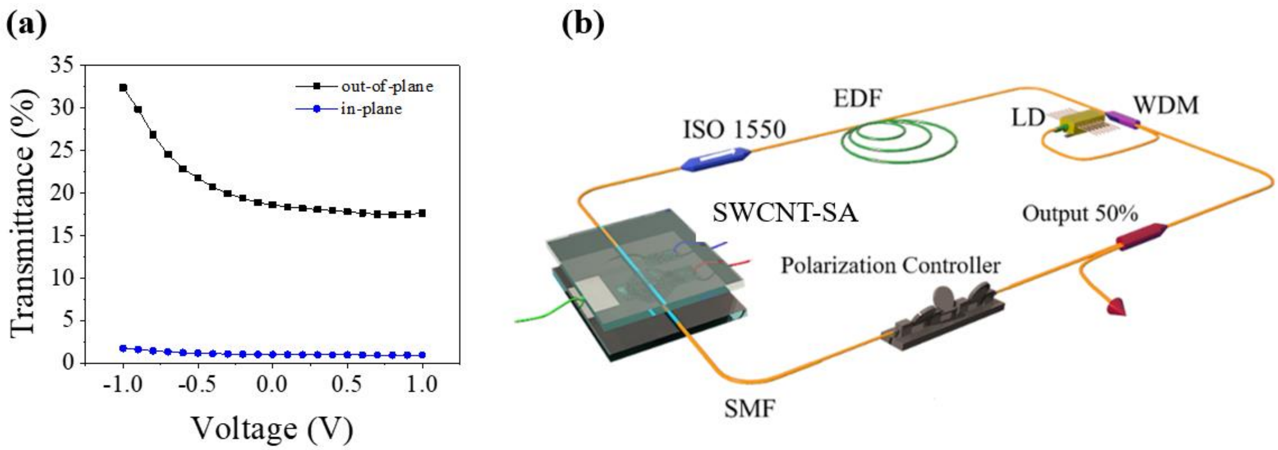

Figure S4. (a) Transmittance curves of the electrically gated SWCNT-SA employing a non-PM single-mode fiber, which were measured for the in-plane and out-of-plane light polarizations. (b) Scheme of the laser without polarization maintaining.

The scheme of the laser without polarization maintaining is shown in Figure S4b. We used 10 meters of erbium-doped fiber (EDF MP980-II) with dispersion crossing zero at 1555 nm. It was pumped by laser diode (LD) at 980 nm through wavelength division multiplexer (WDM). The EDF was followed by a 50% output coupler, polarization controller, gated SWCNT-SA and optical isolator (ISO). The full length of the resonator was 20 m and the net dispersion was -0.25 ps^2. At zero voltage continuous wave generation started at 12 mW of the pump power. With appropriate position of the polarization controller mode-locking self-started at 18 mW in a single-pulse regime. It changed to a multi-pulse regime when the pump power was increased to 26 mW. By applying the negative voltage to the SWCNT-SA, the mode-locked regime could be switched. Under pump power below 40 mW the mode locking switched to the continuous wave generation. If the pump power exceeded 40 mW the multi-pulse mode locking switched to the Q-switched regime. Figure S5 shows the optical spectrum and the pulse train for the mode-locked (a, b) and Q-switched (c, d) regimes.

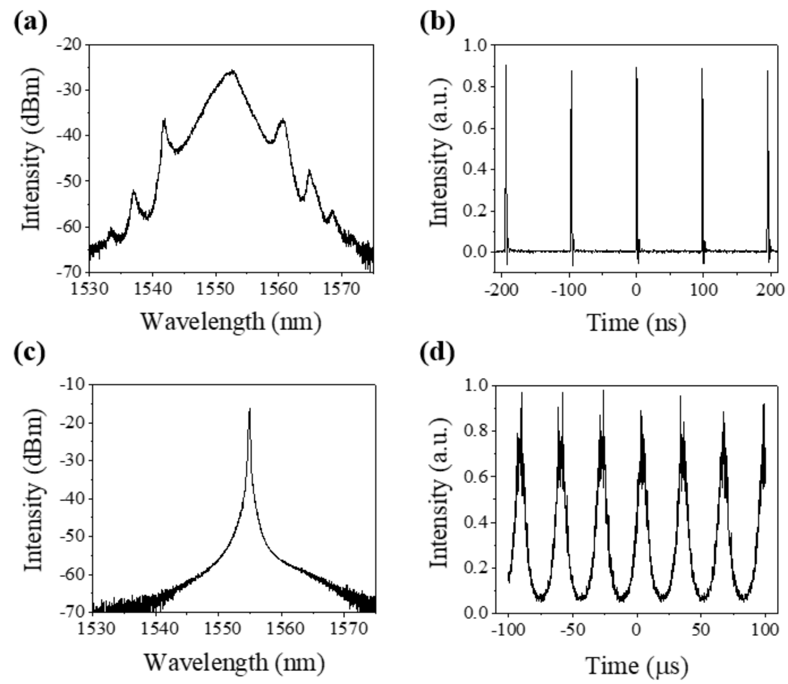

Figure S5. Mode-locking: (a) Optical spectra and (b) pulse trains for zero gate voltage. Q-switched regime: (c) Optical spectra and (d) pulse trains for a gate voltage of -0.8 V.

For this laser we found a strong dependence of the switching conditions on the initial lasing state. The voltage necessary for the pulse regime switching can be adjusted by the polarization controller. Depending on its position pulse generation regimes can be switched at different voltages in a wide range of values. It indicates on the contribution of the nonlinear polarization evolution (NPE) mechanism facilitated by the strong polarization-dependent losses of the SWCNT-SA sample. We conclude that both NPE and SWCNT absorption saturation governs the pulse shaping in the laser based on non-PM SMF. To eliminate the effects of NPE, the all-PM laser scheme is considered in the main text of the article.

S.6 Autocorrelation function measurement

The autocorrelation function of pulses was measured by the APE pulseCheck autocorrelator with scanning range from 120 fs to 150 ps. The laser output pulses were pre-amplified in a home-made fiber amplifier to match their power with the sensitivity of the autocorrelator. The measured autocorrelation function was fitted by the standard formula assuming the sech^2 pulse envelope:

$$A^{(2)}(\tau) = \frac{3}{\sinh^2\left(\frac{2.7\,\tau}{\Delta\tau_A^{FWHM}}\right)}\left[\frac{2.7\,\tau}{\Delta\tau_A^{FWHM}}\coth\left(\frac{2.7\,\tau}{\Delta\tau_A^{FWHM}}\right) - 1\right],$$

where $\Delta\tau_A^{FWHM}$ is a pulse autocorrelation width at half maximum which is connected to the pulse width, $\Delta\tau_p^{FWHM}$, according to the formula $\Delta\tau_A^{FWHM} = 1.54\,\Delta\tau_p^{FWHM}$.

S.7 SWCNT-SA nonlinear optical transmittance

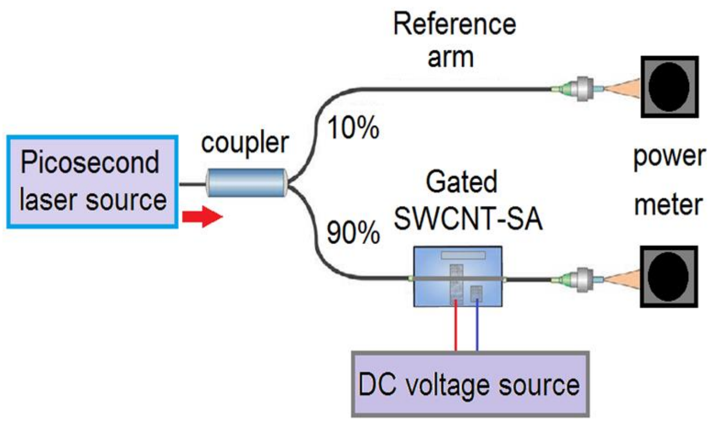

Figure S6. Setup scheme for nonlinear optical transmittance measurements.

We have measured the nonlinear optical transmittance of the gated SWCNT-SA sample under different gate voltages (namely, 0 V, 0.5 V, 0.7 and 1 V). The transmission curves of the SWCNT-SA were retrieved by a common method [1], using a home-made all-PM fiber-based two-arm setup with synchronous dual-channel power measurement (Figure S6). The ultrashort pulse laser source in the setup is comprised of a passively mode-locked Er-fiber-based master oscillator (similar to [2]) and an Er-doped fiber amplifier with tunable gain. This PM laser source delivered near-1-ps pulses with the 48 MHz repetition rate to the input port of a PM fiber coupler. Its 90% output fiber port was cross-spliced with the input fiber of the studied SWCNT-SA. The average laser power available at the input of the studied sample was up to 225 mW. The 10% output fiber port of the coupler formed the reference arm in the measurement setup. The average power was measured in both arms synchronously by a dual-channel power meter using twin power sensor heads (Thorlabs S132C with neutral density filters). To retrieve the main parameters of the saturable absorber we performed curve fitting for measured nonlinear transmittance with the standard function applicable for fast saturable absorbers [3]:

$$T(W) = 1 - A - B\frac{1}{\sqrt{\alpha(1+\alpha)}}\mathrm{atanh}\left(\sqrt{\frac{\alpha}{1+\alpha}}\right),$$

where $\alpha = W/2P_A\tau$, W is the pulse energy, P_A is the saturation power, τ is the pulse width, A gives non-saturable losses and B is the maximum amount of saturable absorption. The results of the fitting of the curves in Figure 6b are summed up in Table S1.

Table S1. Fitting parameters for the nonlinear transmittance measured at different gate voltages.

	0 V	0.5 V	0.7 V	1 V
A	0.558 ± 0.003	0.554 ± 0.005	0.550 ± 0.004	0.560 ± 0.004
B	0.204 ± 0.003	0.204 ± 0.005	0.185 ± 0.003	0.107 ± 0.004
P_A, W	1591 ± 49	1542 ± 88	1691 ± 67	1690 ± 130

[1] Sobon, G., Duzynska, A., Świniarski, M., Judek, J., Sotor, J., & Zdrojek, M. CNT-based saturable absorbers with scalable modulation depth for Thulium-doped fiber lasers operating at 1.9 µm. Scientific reports, 7, 45491, (2017);

[2] S.Kobtsev, A.Ivanenko, Y.G.Gladush, B.Nyushkov, A.Kokhanovskiy, A.S.Anisimov, A.G.Nasibulin. Ultrafast all-fibre laser mode-locked by polymer-free carbon nanotube film. Optics Express, Vol. 24, Issue 25, pp. 28768-28773 (2016);

[3] Schibli, T. R.; Thoen, E. R.; Kärtner, F. X.; Ippen, E. P. Suppression of Q-Switched Mode Locking and Break-up into Multiple Pulses by Inverse Saturable Absorption. *Appl. Phys. B Lasers Opt. 70* (SUPPL), 41–49 (2000).